

2014

# The Feasibility of Creating a 3D Digital Skeletal Collection for Research Purposes and Museum Use

Karen Leigh Beebe

*Louisiana State University and Agricultural and Mechanical College*, bluessence@gmail.com

Follow this and additional works at: [https://digitalcommons.lsu.edu/gradschool\\_theses](https://digitalcommons.lsu.edu/gradschool_theses)



Part of the [Social and Behavioral Sciences Commons](#)

---

## Recommended Citation

Beebe, Karen Leigh, "The Feasibility of Creating a 3D Digital Skeletal Collection for Research Purposes and Museum Use" (2014). *LSU Master's Theses*. 4085.

[https://digitalcommons.lsu.edu/gradschool\\_theses/4085](https://digitalcommons.lsu.edu/gradschool_theses/4085)

This Thesis is brought to you for free and open access by the Graduate School at LSU Digital Commons. It has been accepted for inclusion in LSU Master's Theses by an authorized graduate school editor of LSU Digital Commons. For more information, please contact [gradetd@lsu.edu](mailto:gradetd@lsu.edu).

THE FEASIBILITY OF CREATING A 3D DIGITAL SKELETAL COLLECTION FOR  
RESEARCH PURPOSES AND MUSEUM USE

A Thesis

Submitted to the Graduate Faculty of the  
Louisiana State University and  
Agricultural and Mechanical College  
in partial fulfillment of the  
requirements for the degree of  
Master of Arts

in

The Department of Geography and Anthropology

by  
Karen Leigh Beebe  
B.A., Millsaps College, 2008  
May 2014

## Acknowledgements

First and foremost, I would like to thank my advisor, Heather McKillop, who introduced me to 3D scanning and encouraged me every step of the way. I would also like to thank my committee members, Robert Tague and Rebecca Saunders, for their insightful comments on earlier drafts of this thesis.

Additional thanks goes to Louisiana State University and my advisor's Digital Imaging and Visualization in Archaeology (DIVA) Lab for making this project possible. I am grateful to fellow DIVA lab staff: Valerie Feathers, Victoria Harrington-Burns, Jana Brady, and Lucy Hochstein. I especially thank Valerie for helping me take photographs of the bones, Victoria for screenshots of the 3D models, Jana for her ability to make me laugh, and Lucy for patiently listening to me and offering words of encouragement.

Also, I would like to extend my gratitude to Heather "Bear" Moats, Ashley "Turtle" Franklin, Jacob Jesch, Matthew Chouest, and Heather Marie Brown for all of their advice during my practice thesis defense. Ashley and Heather M. have been a source of love and support during the past two years. I want to thank Todd Brown for his patience and help regarding my nitty-gritty computer questions. I haven't forgotten my DKBFF, Chris Uihlein, who has seen me through the highs and lows of graduate school and the anxieties of working on this project. I also want to thank Tre Pepper for turning his life upside down to support me and my decision to attend graduate school. I will be forever indebted to him.

Finally, I am so grateful to my mother and father for believing in me and teaching me to never give up. Mom, thank you for proofing every single paper I have written since undergrad, including this paper. Also, I must thank Isis for being a constant source of love and knowing the exact moment I needed to snuggle.

# Table of Contents

Acknowledgements .....	ii
List of Tables .....	iv
List of Figures .....	v
Abstract .....	vii
Introduction .....	1
What is 3D Scanning and How Does it Work? .....	2
The NextEngine .....	2
Literature Review .....	5
Moho Cay and Wild Cane Cay .....	5
3D Scanning .....	6
Using 3D Scanning Technology to Create and Study Cross-Sections of Bone .....	7
The Accuracy and Reliability of 3D Scanning .....	7
Measuring Entheses Using 3D Imaging Technology .....	8
Repeatability and Precision of Measurements Taken from 3D Models .....	9
3D Scanning, Virtual Worlds, and Cultural Heritage .....	10
Data Access, File Sharing, and Portability of 3D Scanners .....	11
Methodology .....	13
Results .....	15
Scanning .....	15
Point Experiment .....	36
Visibility of Features .....	39
Discussion .....	40
Learning Curve of 3D Technologies .....	40
Limitations of 3D Scanning .....	41
Benefits of 3D Scanning and 3D Digital Archives .....	43
Conclusions about Feasibility .....	44
Conclusion .....	45
References .....	46
Vita .....	48

## List of Tables

1. Time Required for NextEngine Scan Modes .....	4
2. List of Bones and Visible Features per Bone .....	14
3. Computer Specifications .....	15
4. Time Spent Scanning and Post-Processing Each Bone .....	37
5. Points per Square Inch .....	38
6. Point Experiment .....	39
7. ScanStudio HD System Requirements .....	43

## List of Figures

1. The NextEngine .....	3
2. Right femur, posterior proximal portion .....	16
3. Right femur, distal lateroposterior view .....	16
4. Right femur, posterior proximal portion .....	17
5. Right radius, distal anterior, medial, and lateral views .....	19
6. Right radius, lateroanterior, medial, and medioposterior views .....	20
7. Right radius, proximal superior view .....	21
8. Left ulna, proximal anterior and lateroanterior views .....	22
9. Left ulna, anterolateral and medial aspects .....	22
10. Left humerus, proximal anterior, anteromedial, and posterolateral views .....	24
11. Left humerus, distal anterior and posterior views .....	25
12. Left talus, dorsal and plantar views .....	26
13. Left capitate, lateral and medial views .....	27
14. Left capitate, dorsal and palmar views .....	28
15. Axis, anterior and superior views .....	29
16. Axis, inferior view and posterior is down .....	30
17. 3D model of axis .....	31
18. Axis, posterosuperior view .....	31
19. Right ulna, proximal, anterior, and medial views .....	32
20. Right ulna, distal medial, anterior, and lateral views .....	33
21. Right ulna, distal inferior view .....	34
22. Right third metacarpal, dorsal and lateral views .....	35

23. Right third metacarpal, palmar and medial views .....	35
24. Left scaphoid, palmar is up .....	36

## **Abstract**

3D scanners offer many advantages to scientists and museum curators, such as a permanent digital archival record of the scanned object, the non-intrusive nature of 3D laser surface scanning, the ability to create and share a digital collection with other researchers, and the portability of recent scanners. With the purpose of determining the feasibility of creating a 3D research collection in mind, I have scanned and studied skeletal material from Wild Cane Cay and Moho Cay, Belize. I explore how the 3D model compares to the physical bone and the significance of 3D imaging to the anthropological community.



## Introduction

In the Digital Imaging and Visualization in Archaeology (DIVA) Lab, Dr. Heather McKillop and her students scan archaeological artifacts (e.g., ceramics, wooden posts, flint blades, and skeletal material) using the NextEngine Desktop 3D Scanner HD (model 2020i). Some artifacts are printed in a three-dimensional (3D) printer, and some printed models are painted to be put on display as replicas of the scanned artifact (McKillop and Sills 2013a, 2013b). As part of my graduate assistantship responsibilities, I was assigned to the DIVA Lab where I learned the world of 3D scanning. Based on my experience in the DIVA Lab and published research (Davies et al. 2012; Kuzminsky and Gardiner 2012; Noldner and Edgar 2013; Sholts et al. 2010; Sumner and Riddle 2009), 3D scanning is a time-consuming activity. Nonetheless, the Smithsonian has begun the task of digitizing approximately 10% of their collections in 3D. The Director of the Smithsonian Digitization Program Günter Waibel (2013) explains the challenge for Smithsonian's digitization team: "at 137 million objects, artworks and specimens, capturing the entire collection at a rate of 1 item per minute would take over 260 years of 24/7 effort."

Considering the time-consuming nature of 3D scanning, I ask the following questions: Is creating a digital archive of a skeletal collection a feasible task? Additionally, structures on the bone, such as muscle insertion sites as discussed in the literature review, are important aspects of osteological, bioarchaeological, and forensic research. With that knowledge in mind, are such features evident on the 3D model? If so, are they usable for research? How does the shape of the physical bone compare to the 3D model?

## **What is 3D Scanning and How Does it Work?**

Surface scanners record the contour of an object's surface. Depending on the scanner, the color of an object or its texture also might be recorded. The recorded surface data create a 3D virtual model of the scanned object. Contact scanners and contact-free scanners are the two approaches to surface scanning. My research utilizes a contact free-scanner, which is a system that uses light or laser light reflections to produce a point cloud of the object's surface geometry (Weber and Bookstein 2011:95). A point cloud is a collection of data points, which are typically defined by x, y, and z coordinates in a 3D coordinate system. A point cloud renders the image of a scanned object's surface. Point clouds are converted into models comprised of polygon mesh or triangle mesh. The scanning system used in the present study (the NextEngine) is a triangulation scanner.

Weber and Bookstein (2011:99) explain the triangulation technique as follows:

. . . with the triangulation method the laser light is emitted by the transmitter and simultaneously the receiver (camera) measures where the laser dot is actually located on the object. The laser source, the projected laser dot on the object, and the sensor element of the camera form a triangle, hence the name of the technique.

### **The NextEngine**

The NextEngine scanner is connected to an AutoDrive (a turntable) via a built-in cable, which is plugged in at the front of the scanner to what looks like a telephone line port (see Figure 1). Connected to the turntable is a horizontally adjustable platform on which the scanner operator can place objects to be scanned; the objects are held securely in place with a part-gripper. The part-gripper is important for fragile material (such as archaeological skeletal remains).

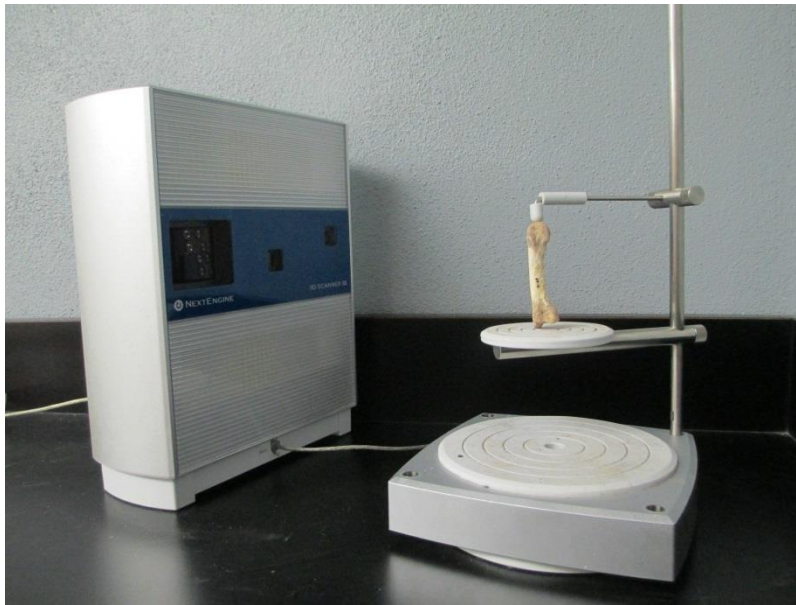


Figure 1. The NextEngine Desktop 3D Scanner HD (left) and the AutoDrive (right)

When the scanning starts, a procedure similar to taking a photograph of the object's surface occurs first. Then, polygons are formed by capturing data points of the object's surface with four slow-moving laser beams. A mesh surface is then created by thousands of polygons that follow the contours of the object, which results in a 3D image. A high-resolution digital color camera is built into the scanner, which collects the color information of the object being scanned. The NextEngine offers three different scan modes: 360-degree, single, and bracket. When the scanner operator selects the 360-degree mode, the number of divisions chosen determines the degree of rotation between scans as well as the total number of scans. For example, if the scanner operator chooses eight divisions, the object will be scanned eight times at 45-degree increments. The eight individual scans are grouped together and referred to as a "scan family." In this mode, the minimum number of divisions is four, and the maximum is sixteen. In the bracket mode, the base will rotate and scan three times. Like the 360-degree mode, these three scans are grouped together as a

scan family. Also in bracket mode, the number of divisions determines the degree of rotation between scans. In 360-degree mode, the number of divisions affects the time required to complete a 360-degree scan (see Table 1). Conversely, the time required to

Table 1. Time Required for NextEngine Scan Modes

Divisions	Scan Mode	Time Required
7	360°	23 minutes
8	360°	27 minutes
9	360°	30 minutes
10	360°	34 minutes
-	Single	3.4 minutes
-	Bracket	10.2 minutes

scan in bracket mode is fixed and not affected by the number of divisions. In single mode, the base performs a single rotation. The number of divisions has no effect in single mode.

Objects can be scanned using two different ranges: macro and wide. In macro range, the object must be a minimum distance of 5 inches from the NextEngine and a maximum distance of 9 inches. The ideal distance in macro range is 6.5 inches. In wide range, the object must be no less than 15 inches and no more than 22 inches from the NextEngine with an ideal distance of 17 inches. According the manufacturer’s website, macro range has an accuracy of 0.005 inches, and wide range has an accuracy of 0.015 inches (<http://www.nextengine.com/faq#accuracy>). Lastly, the NextEngine offers several definition settings: high HD, medium HD, low HD, high STD, medium STD, low STD, high QUICK, medium QUICK, and low QUICK. These definition settings affect the resolution of the scan, scanning time, and storage requirements.

## Literature Review

### Moho Cay and Wild Cane Cay

Moho Cay and Wild Cane Cay are two ancient Maya island sites located along the coast of Belize (McKillop 2004, 2005). Moho Cay functioned as a major trading port from the Late Preclassic through the Postclassic (McKillop 2004, 2005). The Moho Cay Maya were involved in “inland trade of marine resources and ritual paraphernalia from the sea” (McKillop 2004:269). Wild Cane Cay was also a major trading port that operated during both the Classic and Postclassic periods (McKillop 2005). During the Classic period, the Maya of Wild Cane Cay “provided seafood, salt, and ritual items from the sea to inland cities” (McKillop 2005:48). Postclassic Wild Cane Cay is notable for its obsidian trade (McKillop 2005:48, 142).

In addition to being trading ports, Moho Cay and Wild Cane Cay were also ancient Maya island communities (McKillop 2004, 2005). Deceased individuals were found interred under house floors at both sites (McKillop 2004, 2005), which is a burial practice common among the ancient Maya (McKillop 2005). During her Moho Cay excavations, McKillop (2004) unearthed eight burials. McKillop (2004:262) notes the following:

The association of post molds and floors with burials indicates that bodies were interred either on the floor of buildings prior to their renovation or else pits were dug into floors for internments. The burial fill consisted of household midden deposits that contained pottery sherds, chert, obsidian, and faunal remains.

The associated burial ceramics date the Moho Cay burials to the Late Classic period (McKillop 2004:262). During her fieldwork at Wild Cane Cay, McKillop (2005) excavated fifteen burials in Fighting Conch mound. The dead had been interred “in the coral

foundations during structural rebuilding” (McKillop 2005:65), which indicates that these burials “likely marked the deaths of members of the ruling lineage at the island trading port” (McKillop 2005:65). In contrast, the skeletal remains at Moho Cay were found in a brown clay-silt (McKillop 2004). Most of the Wild Cane Cay population “lived in houses made from perishable materials without stone foundations” (McKillop 2005:84).

Radiocarbon dating of charcoal recovered from the floors and associated burial ceramics place the Wild Cane Cay burials during the Postclassic period (McKillop 2005).

### **3D Scanning**

Many of the published articles on 3D scanning methods are technically written and statistic-laden, which can make some of these articles difficult to follow. Kuzminsky and Gardiner (2012) acknowledge this fact and provide their readers with an easy-to-read version of 3D scanning methods. Using simple terminology, Kuzminsky and Gardiner (2012) discuss 3D scanning and introduce the NextEngine scanner, benefits for museum conservation, published research that utilizes 3D models, collaborative efforts, and even the restrictions of 3D scanning. As listed by Kuzminsky and Gardiner (2012:2750), some of the constraints of laser scanning are the following: Laser scanning only captures the surface data; the accuracy of a 3D model depends on the 3D system, software, and scanning operator; scanning can be time-consuming; long-term data storage can be an issue.

Specifically, Kuzminsky and Gardiner (2012) focus on the benefits of 3D imaging within bioarchaeology, forensic anthropology, and museum curation. According to Kuzminsky and Gardiner (2012:2745), the NextEngine “meets many requirements for the purposes of museum conservation and addressing research questions in the fields of biological and forensic anthropology.” Kuzminsky and Gardiner (2011:2745) note some of

the research potential of a completed 3D model includes assessing surface area, volume, and angles; precisely measuring the digital model; digitally reconstructing fragmented bones; and using 3D printed models to create an anatomical skeleton without any destruction to the original skeletal material.

### **Using 3D Scanning Technology to Create and Study Cross-Sections of Bone**

To evaluate biomechanical properties of bone, methods such as CT scanning, biplanar radiography, and periosteal molding techniques are frequently used. Davies et al. (2012) use a 3D laser surface scanner to quantify the cross-sectional geometric properties of long bone diaphyses. The bones used in their study were scanned on a NextEngine 3D laser scanner, processed in ScanStudio, oriented in RapidWorks, and run through AsciiSection to assess biomechanical properties. Available for free online (<http://www.pave.bioanth.cam.ac.uk/software.html>), AsciiSection is a custom-built program written by one of the authors (Davies). Davies et al. (2012) illustrate that the laser scanning method used in their study provides results that are highly correlated to cross-sectional geometric properties obtained through traditional techniques such as periosteal molding and biplanar radiography. Davies et al. (2012:277) conclude that “the AsciiSection method is of comparable if not greater accuracy than traditional molding techniques.”

### **The Accuracy and Reliability of 3D Scanning**

Fourie et al. (2011) assess the accuracy and reliability of anthropometric measurements made with three different 3D systems (Minolta Vivid 900 laser scanner, KaVo 3D exam CBCT scanner, and Di3D stereo-photogrammetry system) and compare the digital measurements to direct physical measurements taken with a set of digital calipers. Fourie et al. (2011:127) use “a series of 21 standardized, linear facial measurements

derived from 15 landmarks taken [. . .] on the face” of seven cadaver heads. Fourie et al. (2011:132) note that “[t]he potential for inter- and intra-observer error is particularly high with 3D laser scanning.” Decisions such as how the object is positioned during scanning, the number of scan rotations, and how multiple scans are merged “can affect the resulting 3D model and its geometric properties, possibly obscuring or distorting meaningful aspects of morphological variation” (Fourie et al. 2011:132). Regardless, Fourie et al. (2011:133) report “no clinical differences when comparing the accuracy and reliability of the 3D anthropometric measurements,” which suggests that the data gathered in their study “are capable of being combined or compared statistically.”

### **Measuring Entheses Using 3D Imaging Technology**

Noldner and Edgar (2013) compare three methods of measuring entheses, including ordinal scoring, 2D measurements, and 3D measurements. The principal hypothesis of Noldner and Edgar’s (2013) study is that the three different methods will not produce the same results concerning entheses development. To test their hypothesis, they examined the humerii, radii, and ulnae from a sample of 24 adult males from the Pottery Mound site in New Mexico. The ordinal method developed by Hawkey and Merbs (1995:329) was used to score entheses where 0 = no expression, 1 = robusticity grade 1 (faint), 2 = robusticity grade 2 (moderate), 3 = robusticity grade 3 (strong). Noldner and Edgar (2013:419) note, “No stress lesions were observed within this sample, so individuals only received scores from 0 to 3. Increments of 0.5 were also used when an entheses’ morphology was intermediate between two main categories.” To determine the 3D surface areas and 2D areas of entheses, Noldner and Edgar (2013) used the NextEngine laser scanner. Before scanning, chalk was applied to the margins of each muscle insertion in order to achieve



better visibility on the digital model. When the scans were complete, the model was cropped so that only the image of the muscle insertion site remained. Then the 3D surface area of the muscle insertion images was measured in ScanStudio HD. To calculate the 2D area of a muscle insertion site, Noldner and Edgar (2013) imported the 3D images into a software program called Rapidform and utilized the program's area measurement tool. Ultimately, Noldner and Edgar (2013:422) report that "3D surface areas and ordinal scores are similar representations of entheses development."

### **Repeatability and Precision of Measurements Taken from 3D Models**

Sholts et al. (2010) examine the repeatability and precision of volume and surface area measurements taken from 3D cranial models. In Sholts et al.'s (2010) study, the NextEngine was used to scan five crania by two scanning operators who used different scanning methods for collecting and processing data. The differences in the two scanning protocols include how the crania was positioned on the AutoDrive, the total number of scans performed of each type of scan (360-degree, bracket, or single), and how many divisions were used. Each cranium was scanned three separate times. Each scanning operator used a mesh triangle size of 0.11-cm, 0.23-cm, and 0.34-cm for the first, second, and third scan, respectively. Measurements were taken in Rapidworks from the final 3D models, which were post-processed in ScanStudio HD PRO. The measurements were used to quantify inter-observer and intra-observer errors and to study possible geometric variation as a result of different scanning methods.

Sholts et al.'s (2010) study produced the following results. First, a more precise measurement of both volume and surface area can be attained from a finer mesh size. Second, despite two separate scanning protocols, the differences in the measurements of

surface area and volume from the resulting 3D models were relatively small. Without standardized methods for calculating surface area and volume, Sholts et al. (2010) argue that one cannot tell whose scanning methods and measurements are more accurate. Finally, Sholts et al. (2010:875) note that the use of a specific scanning protocol would produce highly repeatable results. They suggest that the 3D approach to measuring cranial volume proved more precise than “traditional techniques.”

### **3D Scanning, Virtual Worlds, and Cultural Heritage**

Dawson et al. (2011) take a different approach to 3D technology by using virtual worlds with 3D simulations of indigenous objects and places. Two 3D media projection systems were used in their study: the Java 3D-enabled CAVE Automated Virtual Environment and a Portable 3D Video Wall. Dawson et al. (2011) presented these virtual worlds to Inuit Elders from Kivalliq District and Baffin Region of Nunavut Canada. Wearing 3D glasses, the nine Inuit Elders toured virtual worlds complete with lighting and sound effects that simulated the ambient environment and 3D replicas of archaeological artifacts that had been scanned with a laser scanner. If a viewer selected a specific artifact in this virtual world, the 3D model would appear and rotate slowly so the viewer could see all angles of the object.

Dawson et al. (2011:395) report that during the Elders’ virtual reality tour, the Elders tried to touch the virtual artifacts. Whispering in their native Inuktitut, one Elder said, “It [the virtual world] really makes me think about what it would have been like to live in my ancestors’ home” (2011:395). Another stated, “No one has ever seen these buildings before. Now we are able to and it will help us understand who we are” (2011:395). All of the Elders agreed that future generations of Inuit could benefit from

these virtual worlds. In other words, virtual worlds have the potential to captivate and teach young and computer-literate Inuit about their culture and history.

### **Data Access, File Sharing, and Portability of 3D Scanners**

Archaeological material and osteological collections often are rare and fragile. As a result, preservation of this irreplaceable material is a top priority. The advent of 3D scanning technologies such as CT scans, MRIs, and 3D laser surface scanners can allow a researcher to study a specimen while limiting direct handling of delicate archaeological and osteological material. Gilissen (2009:224) notes that using scanned data could replace, to some extent, the use of “actual collections and hence prevent the degradation of the material.” As previously mentioned, the use of scanning technologies in Anthropological research is recent. Naturally, the issue of data access is a topic in need of attention, but for the purposes of my thesis, I will simply refer to the positive outlook of Sumner and Riddle (2009). Sumner and Riddle (2009:220) address the issue of information sharing in the Digital Age and note – just as Kuzminsky and Gardiner (2012) did – the potential for research collaboration on the global scale. Sumner and Riddle (2009:220) report that the “digital reproduction of artifacts and biological remains has the potential to put data into the hands of far more researchers, in more places, in a more timely and cost-effective fashion than traditional methods of information sharing.” Therefore, Sumner and Riddle (2009) urge the global anthropological community to cooperate with one another and grant fellow researchers greater data access.

Another application of 3D scanning is bringing a 3D scanner to an archaeological site and scanning artifacts or bone at the site. In 2011, paleontologist Nick Pyenson was excavating whale bones in Chile (Tucker 2012) when his colleagues warned him that “the

whole site would be paved over within two months” (Tucker 2012). Pyenson called upon Vincent Rossi and Adam Metallo of the Smithsonian’s 3D Digitization team. Using 3D scanning technology, Rossi and Metallo scanned the whale fossils at the site in Chile so that “scientists could study the site forever” (Tucker 2012). In 2011, 2012, and 2013, a NextEngine 3D Scanner from the LSU DIVA Lab was taken to Belize to image ancient Maya waterlogged wood and pottery artifacts from ongoing excavations of Paynes Creek salt (McKillop and Sills 2013a, 2013b). Some of the 3D scans were post-processed at LSU in the DIVA Lab with 3D printed replicas made for exhibits in Belize and the USA.

## **Methodology**

The archaeological collections comprising the study sample are ancient Maya skeletal remains from Wild Cane Cay and Moho Cay, Belize (McKillop 2004, 2005). The collections were chosen by my advisor due to my interests in the ancient Maya and skeletal analysis. Ten postcranial bones were scanned from the collections using the NextEngine Desktop 3D Scanner HD, model 2020i (Table 2). NextEngine's accompanying software, ScanStudio HD PRO, was used to trim, align, and fuse the models. Davies et al. (2012:282) illustrate that the accuracy of a scan depends on the NextEngine's scan quality settings. According to Davies et al. (2012), the most accurate setting is high HD.

To explore the feasibility of creating a 3D digital collection of skeletal remains, I documented the amount of time I took to scan and post-process the 3D models. In addition, I made some observations concerning the visibility of features on the bones and on the 3D models (see Table 2). Screenshots of the 3D models were taken in Geomagic Design X 2014 by Victoria Harrington-Burns in the LSU DIVA Lab. In consultation with my advisor, we chose the most complete, non-fragmented bones that represented a range of sizes and elements as a case study. Certain bones for scanning and certain features for observation were not chosen because cortical bone was missing and trabecular bone was exposed to such an extent that I would have been unable to effectively discuss the bones and their characteristics.

Table 2. List of Bones and Visible Features per Bone

List of Bones	Visible Features per Bone	Site	Burial	Catalogue #
axis	dens vertebral and transverse foramina superior articular facets	Moho Cay	4	-
left humerus	crest of the lesser tubercle intertubercular groove coronoid, radial, and olecranon fossae	Moho Cay	4	-
left ulna	ulnar tuberosity interosseous border nutrient foramen	Moho Cay	1	-
right ulna	trochlear notch radial notch ulnar head	Wild Cane Cay	9	13
right radius	radial head radial tuberosity ulnar notch	Wild Cane Cay	7	2
left scaphoid	scaphoid tubercle facet for the head of the capitate radial facet	Wild Cane Cay	9	270
left capitate	head facets nonarticular surfaces	Wild Cane Cay	9	203
right third metacarpal	styloid process facet for capitate facets for MC2	Wild Cane Cay	9	29
right femur	fovea capitis gluteal tuberosity impression for the lateral head of the <i>gastrocnemius</i> popliteal groove	Wild Cane Cay	3	7
left talus	trochlea sulcus tali posterior calcaneal facet	Wild Cane Cay	-	24

# Results

## Scanning

Scanning began with the right femur from Wild Cane Cay burial 3 on the Lenovo desktop in the LSU DIVA Lab (see Table 3 for computer specifications). The process took approximately 20 hours to scan (ten divisions, macro range, medium HD) and align. After the fourth scan family, extra rotations were added to see if twelve divisions would result in less missing data (holes) in the model. The additional rotations did not make a difference in the model's appearance. During the fusing stage, ScanStudio crashed during every attempt to fuse. Unable to fuse the scan families, the model was abandoned. The right femur was rescanned using ten divisions in medium HD. Wide range was used for the first scan family. Subsequent scan families were in macro range. The second attempt was successful (see Figures 2, 3, and 4). The process from first scan through alignment, fusing, and filling holes took a total of 15 hours. However, an airtight model suitable for 3D printing was not achieved. For the other nine models, no further post-processing actions were taken once the model was fused.

Table 3. Computer Specifications

Lenovo Desktop	Samsung Laptop
Windows 7 (64-bit)	Windows 7 (64-bit)
Intel® Core™ i7-3770 CPU @3.40 GHz	Intel® Core™ i7 CPU @1.60 GHz
12.0 GB RAM	8.00 GB RAM
NVIDIA GeForce GT 545	NVIDIA GeForce GT 330M



Figure 2. Right femur, posterior proximal portion. Left: 3D model showing the visibility of the gluteal tuberosity on the 3D image. Right: photograph of physical bone with scale.



Figure 3. Right femur, distal lateroposterior view. Left: 3D model showing discrete features visible on the 3D image. Right: photograph of physical bone with scale.



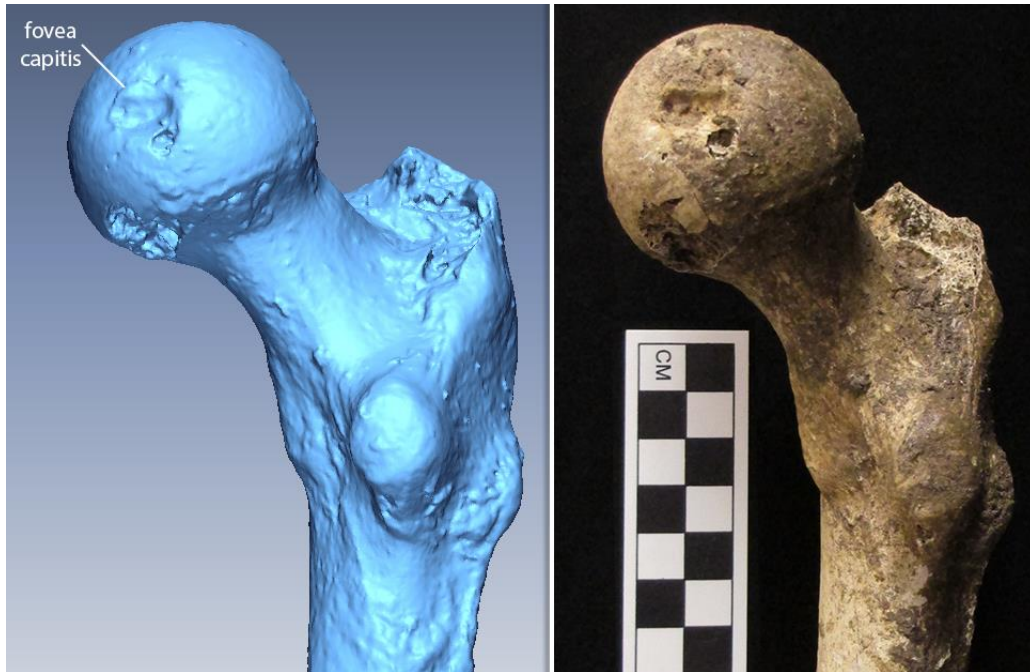


Figure 4. Right femur, posterior proximal portion. Left: 3D model showing the visibility of the fovea capitis on the 3D image. Right: photograph of physical bone with scale.

After an interim of five weeks, scanning was resumed on a different computer, a Samsung laptop (see Table 3 for computer specifications), beginning with the right radius from Wild Cane Cay burial 7. In favor of the most accurate scan quality the NextEngine can offer, high HD was preferred over medium HD. Accordingly, the right radius was scanned using ten divisions, macro range, and high HD. While working on the model of the right radius, the laptop ran slowly; a process that should only take a couple minutes (or less) would take up to ten (or more) minutes. All too often, ScanStudio would stop responding and then crash. Consequently, approximately 14 hours were spent on the first right radius model. Regardless, all of the scan families were successfully fused. Six weeks later, the right radius was rescanned on the Lenovo desktop using seven divisions, macro range, and medium HD. The right radius was rescanned in favor of consistency in using medium HD, to see if the time spent scanning could be improved, and for convenience of having all 3D

models on the same computer. After scanning the second scan family, an observation was made that 3D data were missing along the interosseous border. The third scan family was scanned using eight divisions to see if more rotations were needed to capture the entirety of the interosseous border. However, three scan families of eight, nine, and ten divisions were unable to completely capture the entire interosseous border.

Another observation was made that the positioning of an object on the turn table affected the 3D data captured. For the first five scan families, the narrowly sharp interosseous border of the right radius was facing the camera and lasers at the start of the scan rotations. The radius was repositioned so that the lateral aspect of the radius was the first to be scanned and the interosseous border would be scanned during the middle of scan rotations. The shaft of the radius was scanned in this position using seven divisions. However, there were still missing data along the interosseous border when the scan family completed. Maintaining the same position, the shaft of the radius was rescanned using ten divisions. This set-up was the best attempt at capturing the entirety of the interosseous border. However, a sliver of missing data remained. The final fused 3D model (see Figures 5, 6, and 7) took 6.5 hours to complete.

Following the first complete 3D model of the right radius, the left ulna from Moho Cay burial 1 was scanned on the Samsung laptop. After 4.5 hours of scanning in high HD, macro range, and using ten divisions, an error message stating the scanner was disconnected began to continually appear and disrupt scanning progress. Since I was in the process of scanning, I could not close the scanning program to check the error message. The next time the model was opened, a bug report appeared stating that the file might be corrupted. Unable to reach a solution with ScanStudio technical support, the model was

abandoned. The left ulna was rescanned using the same scan settings (ten divisions, macro range, and high HD). An attempt was made to fuse the model, but ScanStudio continually froze and crashed. During one of the fuse attempts, a low RAM warning appeared, which led to the conclusion that ten divisions in high HD used more memory than the laptop could handle. Therefore, the model was abandoned after a time investment of 9 hours.



Figure 5. Right radius, distal anterior (left), medial (middle), and lateral (right) views. Top: 3D models showing the visibility of the ulnar notch on the 3D image. The red areas indicate missing data or “holes” in the model’s mesh. Bottom: photographs of physical bone with scale.



Figure 6. Right radius, lateroanterior (left), medial (middle), and medioposterior (right) views. Top: 3D models showing discrete features visible on the 3D image. The red areas indicate missing data or “holes” in the model’s mesh. Bottom: photographs of physical bone with scale.

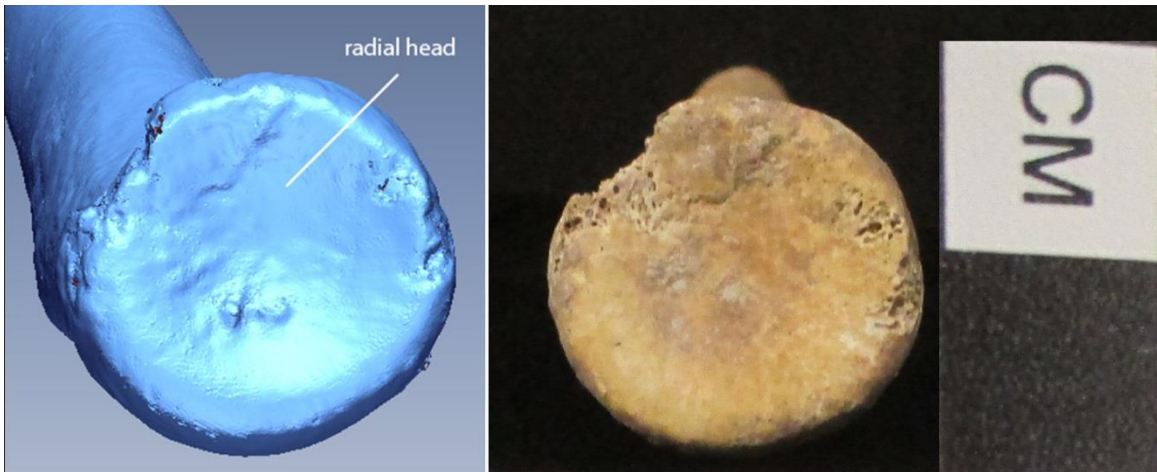


Figure 7. Right radius, proximal superior view. Left: 3D model showing the visibility of the radial head on the 3D image. The red areas indicate missing data or “holes” in the model’s mesh. Right: photograph of physical bone with scale.

The left ulna was scanned for a second time using seven divisions, macro range, and high HD. During the scanning process, the laptop ran a bit more smoothly than when scanned in ten divisions. However, during the alignment process, a global alignment error message appeared preventing the alignment from moving forward. During a second alignment attempt, ScanStudio froze, and the program had to be force-closed. ScanStudio continued to freeze during all subsequent alignment attempts. The model was abandoned, and a third 3D scan was started using seven divisions in macro range and high HD. However, after struggling to complete three scan families, the newest model was discarded.

At this point, an approximate total of 23.5 hours had been spent on scanning and post-processing attempts of the first three models of the left ulna. A week later, scanning resumed of the left ulna on the Lenovo desktop using seven divisions, macro range, and medium HD. Scanning and post-processing went smoothly and without any software issues until the fusing stage. During the first fuse attempt, ScanStudio crashed. The second

attempt to fuse the scan families was successful, which resulted in the final model of the left ulna (see Figures 8 and 9). The entire process of this fourth rescan took 3.5 hours.



Figure 8. Left ulna, proximal anterior and lateroanterior views, respectively. Left: 3D models showing the visibility of the ulnar tuberosity on the 3D image. The red areas indicate missing data or “holes” in the model’s mesh. Right: photographs of physical bone with scale.

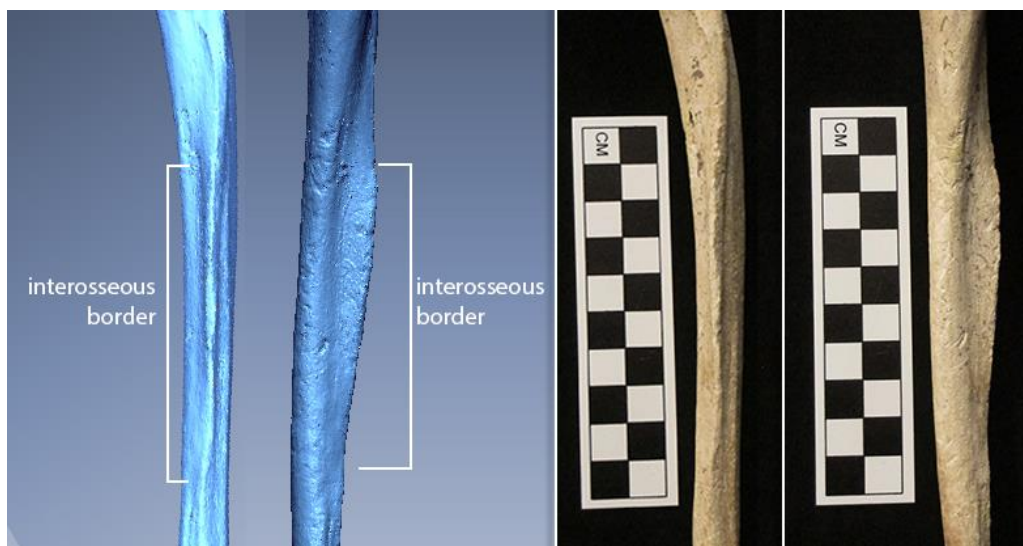


Figure 9. Left ulna, anterolateral and medial aspects, respectively. Left: 3D models showing the visibility of the interosseous border on the 3D image. The red areas indicate missing data or “holes” in the model’s mesh. Right: photographs of physical bone with scale.

After the third rescan of the left ulna was discarded, the left humerus from Moho Cay burial 4 was scanned on the Samsung laptop using seven divisions, macro range, and high HD. As seen in Table 1, a scan with seven divisions in the 360-degree mode takes 23 minutes. When a scan is completed, ScanStudio automatically runs a global alignment. Typically, the global alignment process only takes a minute or less. Switching to high HD causes this process to take an additional 5-12 minutes. Although experienced during the previous high HD scans, this sluggishness became more prominent during the scanning of the left humerus. In addition, an error message appeared during the middle of a scan stating that no 3D data were captured. As a result, ScanStudio cancelled the scan, which had to be restarted. While trimming, the laptop's display driver experienced an error and force-closed ScanStudio. At this point, the combined time for scanning and post-processing should have been one hour. Instead, the process took me 2.6 hours, and the model was not even complete.

The following scan session of the left humerus was rife with ScanStudio complications. The error message stating the scanner was disconnected reappeared and continually disrupted the scanning progress. On the seventh division of seven or right before global alignment, the scanner would "disconnect" and ScanStudio would crash. After two hours, nothing had been scanned. The same issues were experienced during the next scan session, so the model was abandoned. As a result of the escalating technical difficulties, no further scanning was attempted on the Samsung laptop.

Scanning of the left humerus resumed on the Lenovo desktop using seven divisions, macro range, and high HD. The scanning and post-processing stages ran much smoother than on the Samsung laptop. However, once again, ScanStudio crashed during the fusing

stage. Unable to fuse, the left humerus was rescanned with seven divisions, an initial wide range and the remainder in macro range, and medium HD. Again, ScanStudio crashed after trying to fuse the scan families. A week and a half later, a second fuse attempt proved successful, which resulted in the final model of the left humerus presented here (see Figures 10 and 11). The same fuse settings were used during both instances of fusing.

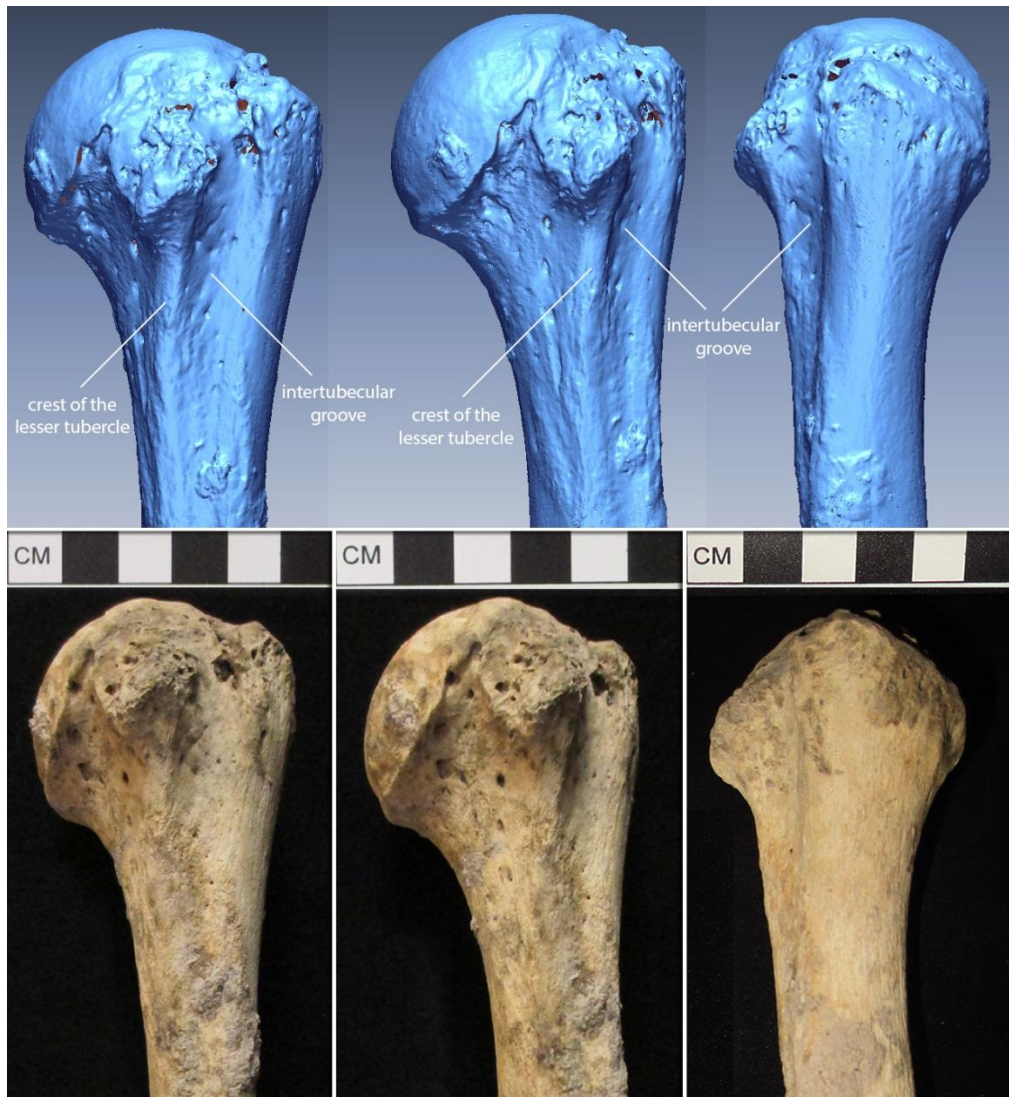


Figure 10. Left humerus, proximal anterior (left), anteromedial (middle), and posterolateral (right) views. Top: 3D models showing discrete features visible on the 3D image. The red areas indicate missing data or “holes” in the model’s mesh. Bottom: photographs of physical bone with scale.



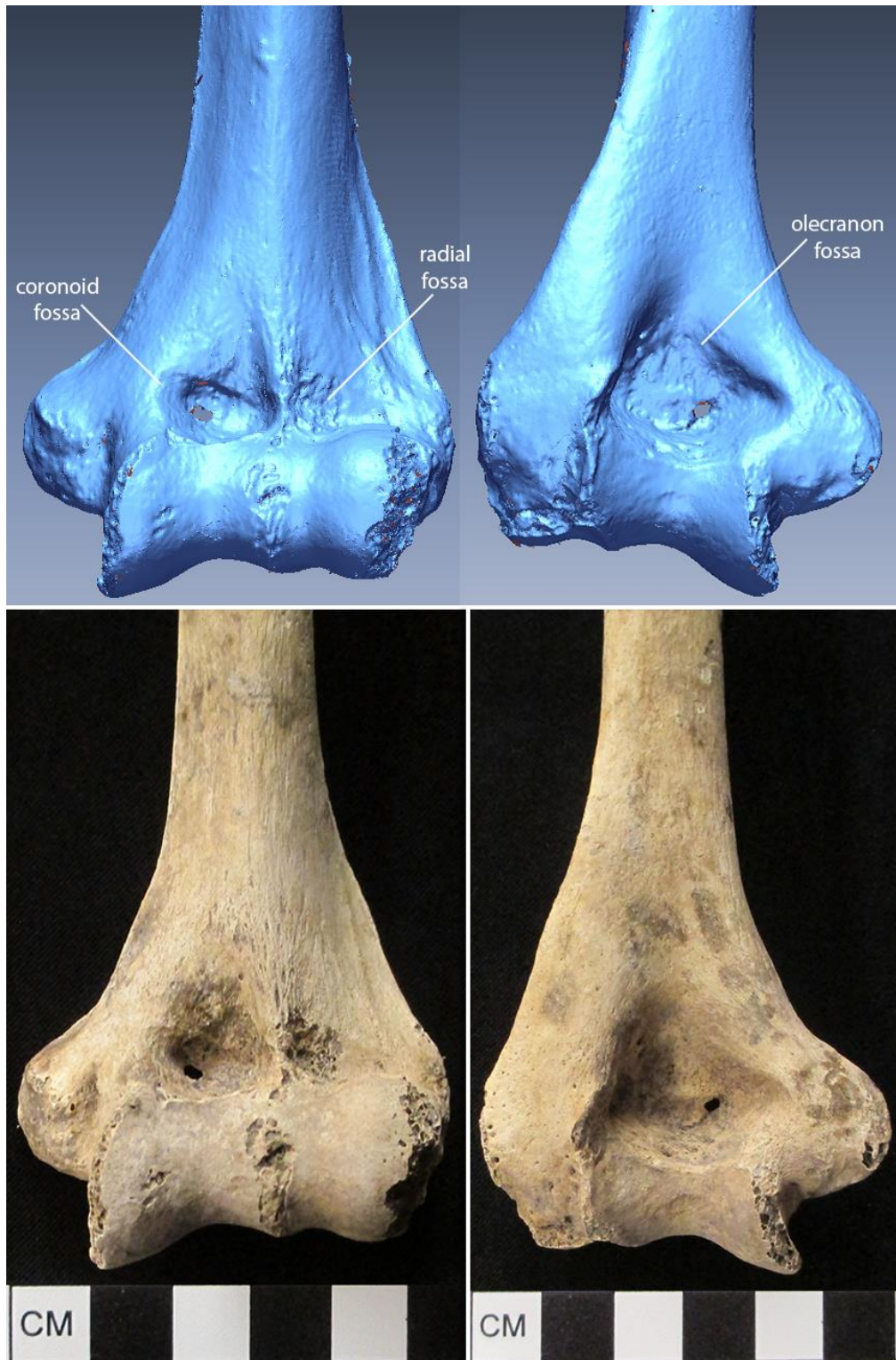


Figure 11. Left humerus, distal anterior (left) and posterior (right) views. Top: 3D models showing discrete features visible on the 3D image. The red areas indicate missing data or “holes” in the model’s mesh. Bottom: photographs of physical bone with scale.

The left talus from Wild Cane Cay was first scanned using seven divisions in medium HD and macro range and completed within 1.5 hours. However, there were a lot of missing data (holes) in the model. Therefore, with the goal of capturing more data, the left talus was rescanned using more divisions (ten divisions, medium HD, macro range). This model was completed within 2.5 hours. Later I edited the scan to include more families because the added divisions were not capturing all of the data. After a series of single scans and a total of 3.25 hours, the second left talus model was abandoned in favor of creating a cleaner model than the previous two. The left talus was rescanned for a second time using seven divisions, medium HD, and macro range. The final model presented in this paper (see Figure 12) took 2.4 hours to complete.



Figure 12. Left talus, dorsal (left) and plantar (right) views. Top: 3D models showing discrete features visible on the 3D image. The red areas indicate missing data or “holes” in the model’s mesh. Bottom: photographs of physical bone with scale.

Scanning of the left capitate from Wild Cane Cay burial 9 began with ten divisions in medium HD and macro range. The second scan family used eight divisions but was rescanned with nine divisions. After alignment of the first two scan families and an additional bracket scan, the left capitate model had overlapping extra data in its crevices. Thus, the left capitate was rescanned using nine divisions, medium HD, and macro range. Once again, the model had overlapping/extra data in crevices seen on its lateral and palmar aspects. As a result, the left capitate was rescanned for a second time using seven divisions, medium HD, and macro range. The model (Figures 13 and 14) was complete in 1.9 hours.

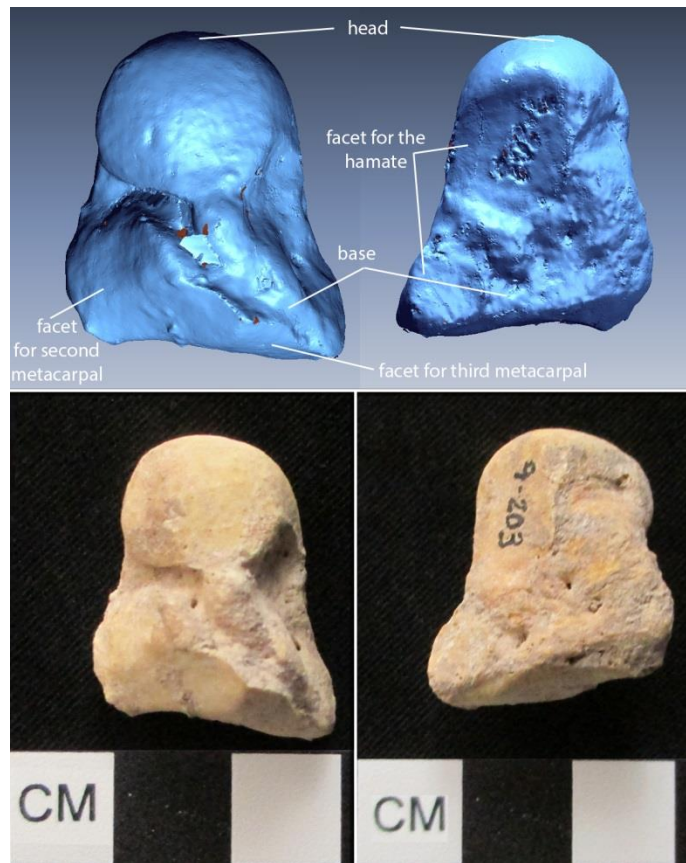


Figure 13. Left capitate, lateral (left) and medial (right) views. Top: 3D models showing discrete features visible on the 3D image. The red areas indicate missing data or “holes” in the model’s mesh. Bottom: photographs of physical bone with scale.



Figure 14. Left capitate, dorsal (left) and palmar (right) views. Top: 3D models showing discrete features visible on the 3D image. The red areas indicate missing data or “holes” in the model’s mesh. Bottom: photographs of physical bone with scale.

The first two scan families of the axis from Moho Cay burial 4 were scanned using seven divisions, medium HD, and macro range. Experiencing difficulty capturing the data around the foramina, the third scan family was scanned with ten divisions. Similar to the left capitate, the axis model had overlapping data as well as “stray” data sticking out of the model. With the thought that perhaps too much data were being captured, the fourth and fifth scan families were scanned with eight divisions instead of ten. Still displaying

overlapping data, the first three scan families were deleted and rescanned using a variation of bracket and single mode to capture the missing data. The first two attempts to fuse the scans were unsuccessful. However, the third 3D scan attempt was successful. The fused model still had areas of missing data. A single scan was added to the model and then fused. The entire process took 7.8 hours. The resulting 3D model is presented in this report (see Figures 15, 16, 17, and 18).

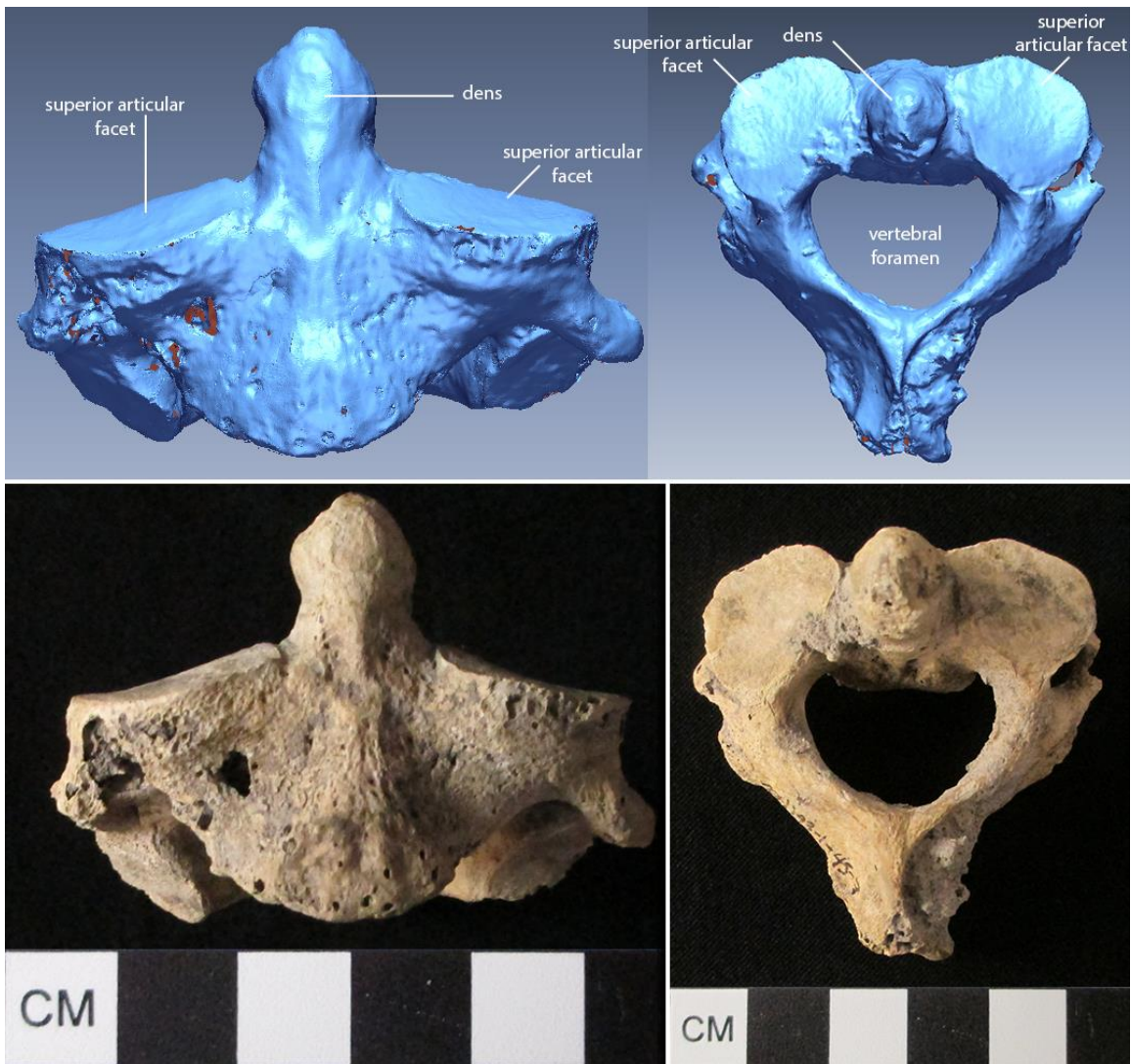


Figure 15. Axis, anterior (left) and superior (right) views. Top: 3D models showing discrete features visible on the 3D image. The red areas indicate missing data or “holes” in the model’s mesh. Bottom: photographs of physical bone with scale.

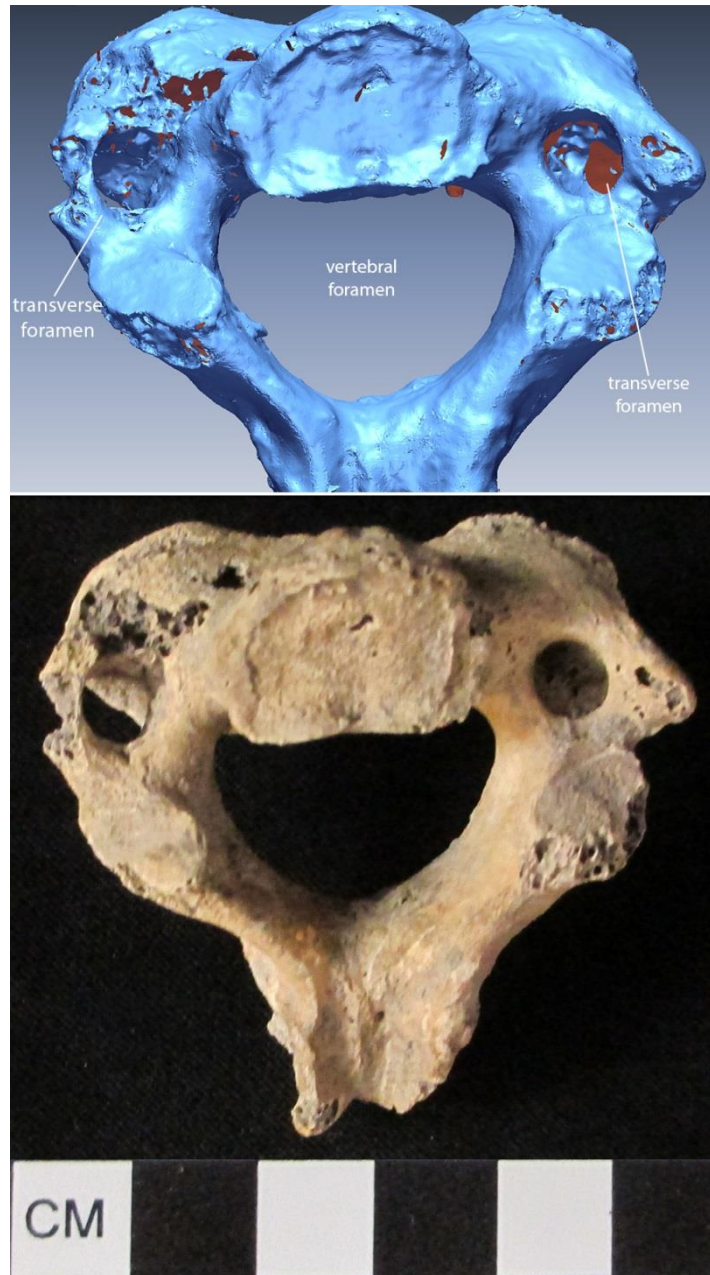


Figure 16. Axis, inferior view and posterior is down. Top: 3D model showing discrete features visible on the 3D image. The red areas indicate missing data or “holes” in the model’s mesh. Bottom: photograph of physical bone with scale.

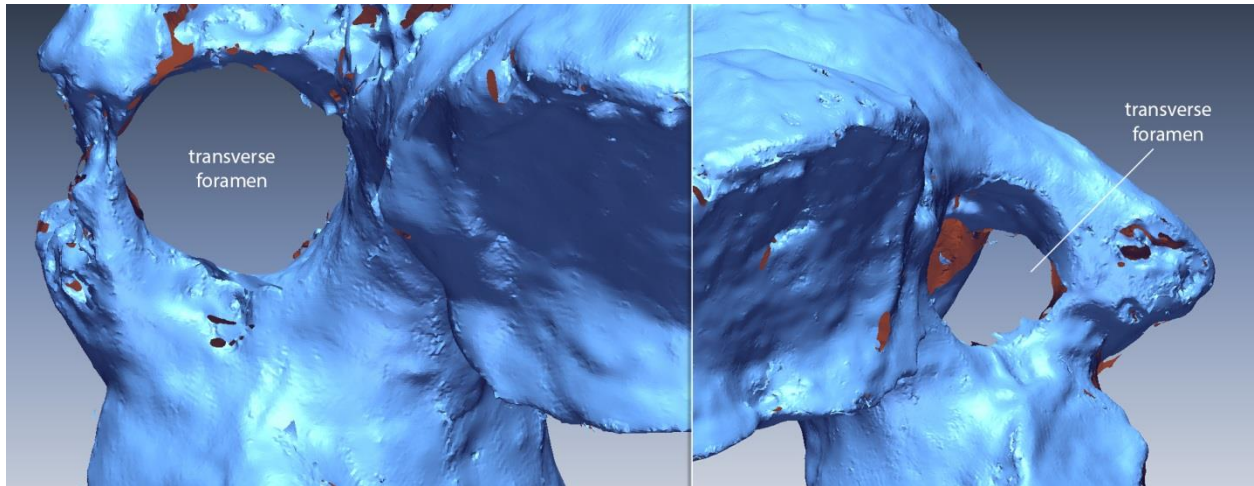


Figure 17. 3D model of axis (inferior view, posterior is down) showing the visibility of the transverse foramina on the 3D image. The red areas indicate missing data or “holes” in the model’s mesh.

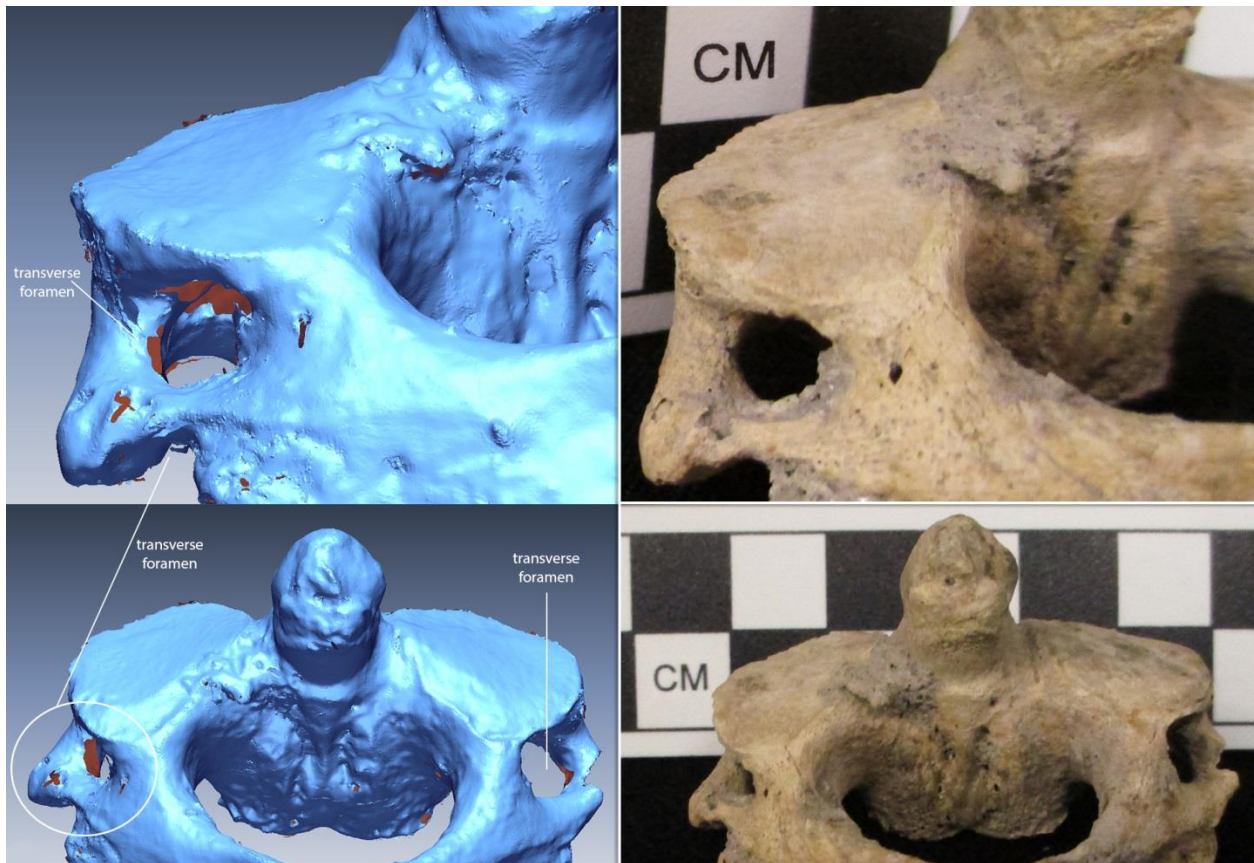


Figure 18. Axis, posterosuperior view. Left: 3D models showing the visibility of the transverse foramina on the 3D image. The red areas indicate missing data or “holes” in the model’s mesh. Right: photographs of physical bone with scale.

The right ulna from Wild Cane Cay burial 9 was scanned using seven divisions, medium HD, and macro range. The only technical issue experienced while working on this model was that the first attempt to fuse was unsuccessful. However, the second attempt to fuse was successful. The total time spent scanning and post-processing the right ulna was 4.3 hours (see Figures 19, 20, 21).



Figure 19. Right ulna, proximal (left), anterior (middle), and medial (right) views. Top: 3D models showing discrete features visible on the 3D image. The red areas indicate missing data or “holes” in the model’s mesh. Bottom: photographs of physical bone with scale.



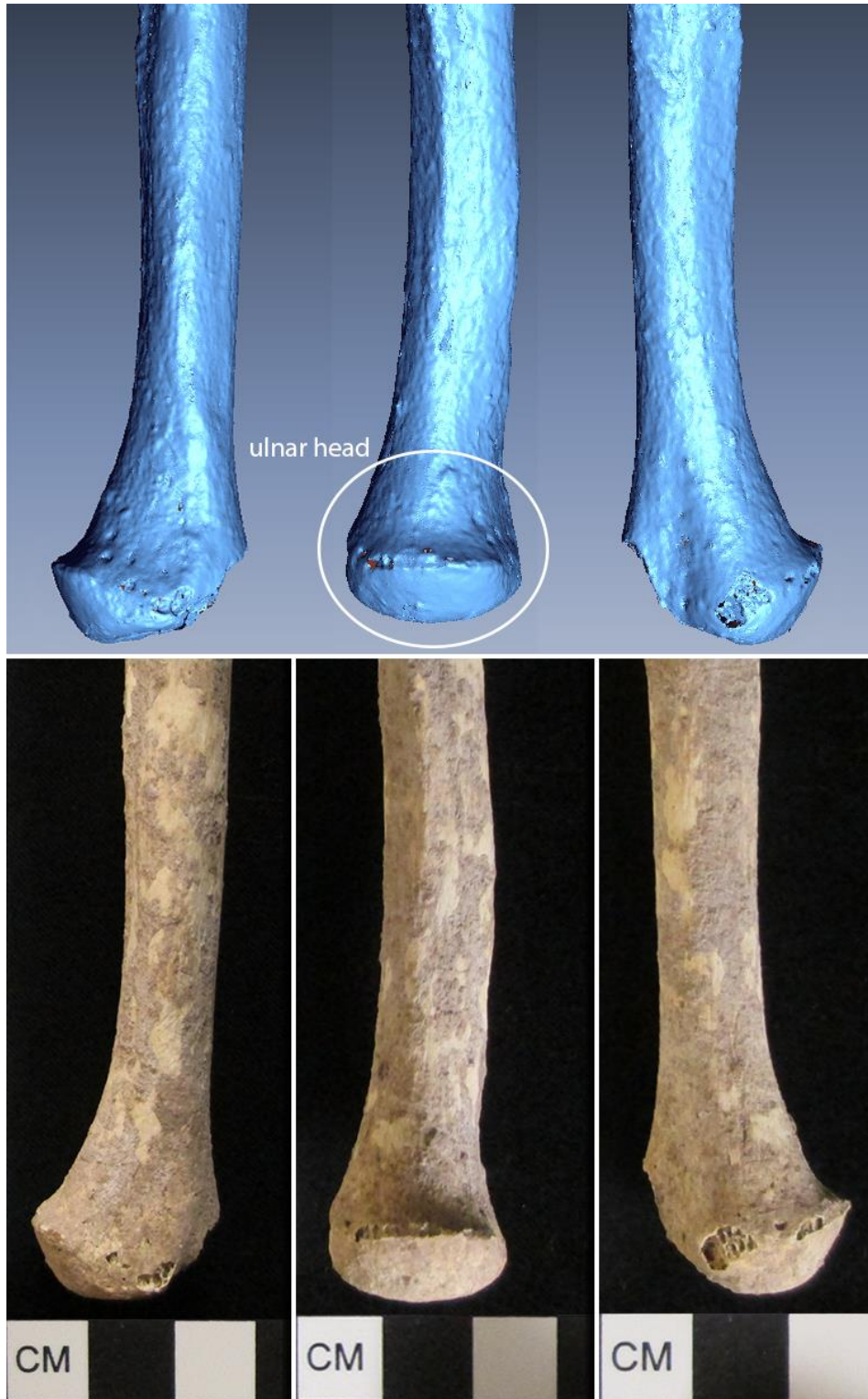


Figure 20. Right ulna, distal medial (left), anterior (middle), and lateral (right) views. Top: 3D models showing the visibility of the ulnar head on the 3D image. The red areas indicate missing data or “holes” in the model’s mesh. Bottom: photographs of physical bone with scale.

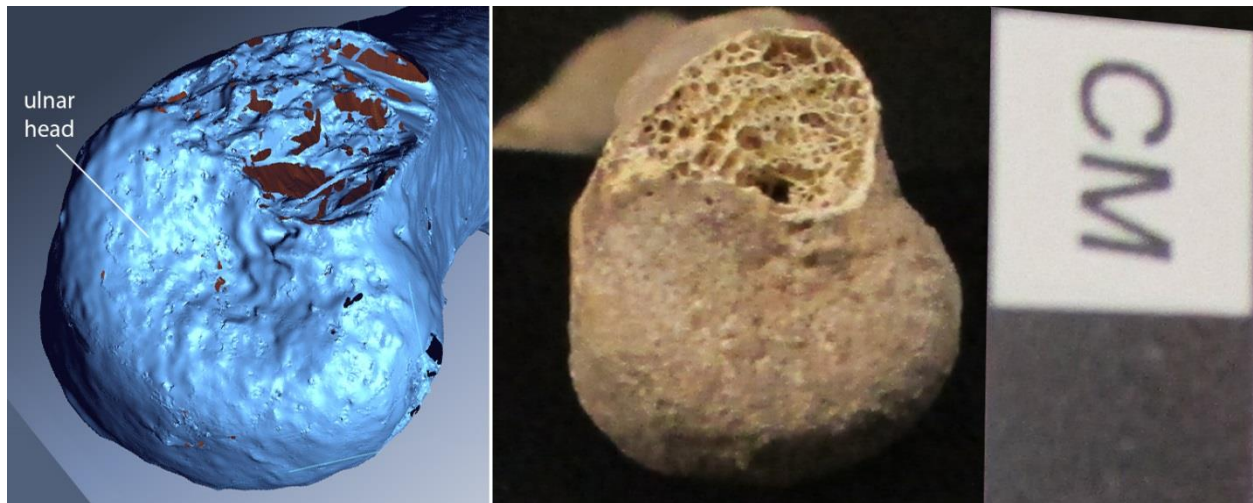


Figure 21. Right ulna, distal inferior view. Left: 3D model showing the visibility of the ulnar head on the 3D image. The red areas indicate missing data or “holes” in the model’s mesh. Right: photograph of physical bone with scale.

The right third metacarpal from Wild Cane Cay burial 9 was scanned using eight divisions in medium HD and macro range. No technical issues were experienced while scanning and post-processing the model for the right third metacarpal. The total time spent on this model (see Figures 22 and 23) was 1.8 hours. Following the third metacarpal was the left scaphoid from Wild Cane Cay burial 9, which was scanned using eight divisions in medium HD and macro range. Again, the computer, scanner, and scanning software ran smoothly. The total time spent scanning the scaphoid model (see Figure 24) was approximately one hour.

Ultimately, most bones in my study were rescanned as a result of a series of unsuccessful fusing attempts or technical difficulties with the computer and/or ScanStudio. On the other hand, some bones were rescanned because the 3D image had large portions of missing data, areas with overlapping or extra data, or the scan generally looked cluttered. See Table 4 below for the time spent scanning and post-processing each bone.

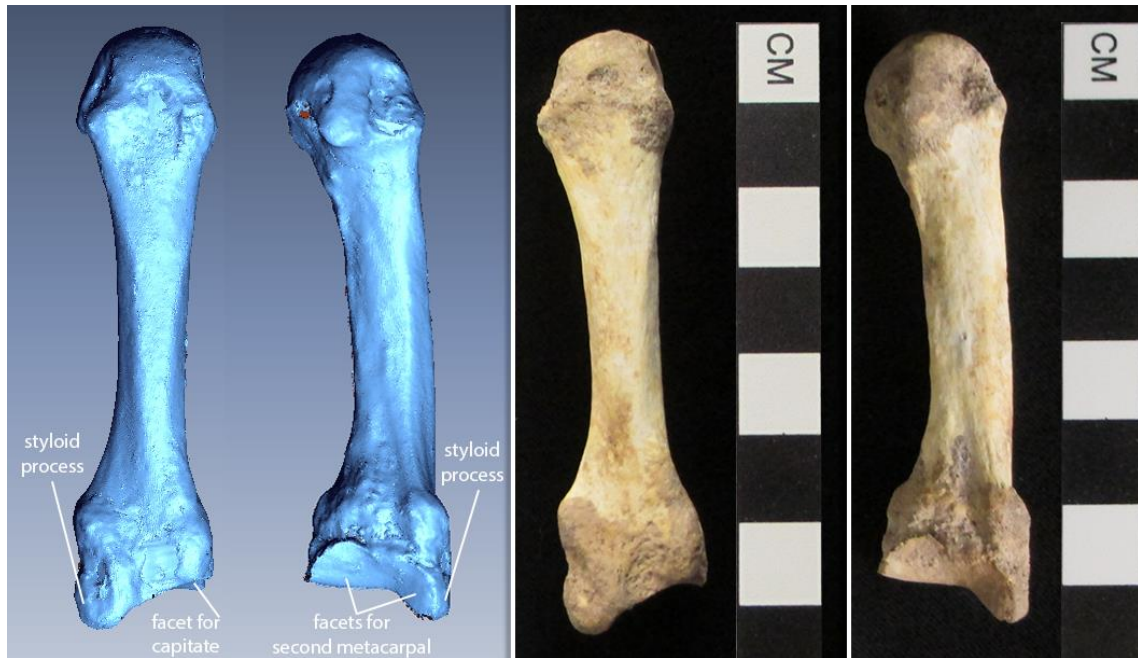


Figure 22. Right third metacarpal, dorsal and lateral views, respectively. Left: 3D models showing discrete features visible on the 3D image. The red areas indicate missing data or “holes” in the model’s mesh. Right: photographs of physical bone with scale.



Figure 23. Right third metacarpal, palmar and medial views, respectively. Left: 3D models showing discrete features visible on the 3D image. The red areas indicate missing data or “holes” in the model’s mesh. Right: photographs of physical bone with scale.

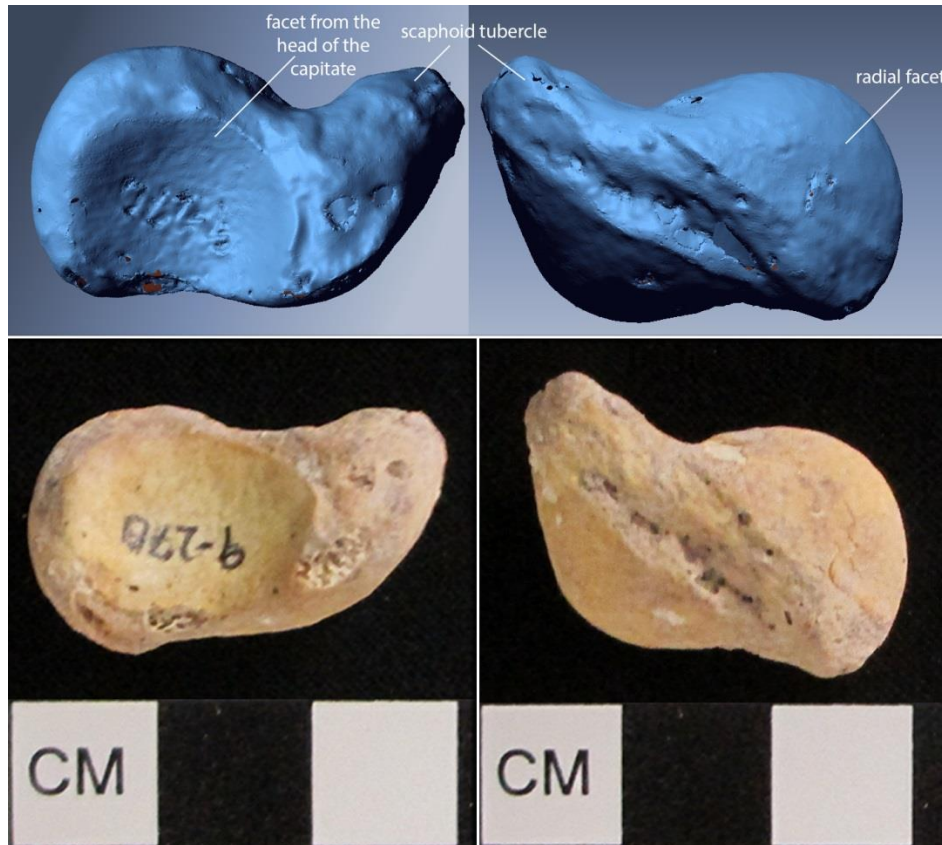


Figure 24. Left scaphoid, palmar is up. Top: 3D models showing a discrete feature visible on the 3D image. The red areas indicate missing data or “holes” in the model’s mesh. Bottom: photographs of physical bone with scale.

### Point Experiment

As mentioned earlier, the NextEngine uses laser light reflections to produce a point cloud of the scanned object’s surface geometry. A point cloud is a collection of data points, which basically renders the image of a scanned object’s surface. When setting the definition and range of a scan, ScanStudio displays the number of points that will be generated per square inch. A scan in high HD and macro range produces 160,000 points per square inch. In contrast, a scan in medium HD and macro range produces 40,000 points per square inch (see Table 5 below). When scanning in high HD, 100% of the computer’s memory is being used. When scanning in medium HD, the amount of memory used is dependent upon the

Table 4. Time Spent Scanning and Post-Processing Each Bone

Bone	Scan Attempt	Divisions	Definition	Range	~Time Spent
right femur	1	10	medium HD	macro	20 hours
right femur	2	10	medium HD	wide/macro	15 hours
<i>Total</i>					35 hours
right radius	1	10	high HD	macro	14 hours
right radius	2	7	medium HD	macro	6.5 hours
<i>Total</i>					20.5 hours
left ulna	1	10	high HD	macro	4.5 hours
left ulna	2	10	high HD	macro	9 hours
left ulna	3	7	high HD	macro	6 hours
left ulna	4	7	high HD	macro	4 hours
left ulna	5	7	medium HD	macro	3.5 hours
<i>Total</i>					27 hours
left humerus	1	7	high HD	macro	4.8 hours
left humerus	2	7	high HD	macro	4.5 hours
left humerus	3	7	medium HD	wide/macro	5.1 hours
<i>Total</i>					14.4 hours
left talus	1	7	medium HD	macro	1.5 hours
left talus	2	10	medium HD	macro	3.25 hours
left talus	3	7	medium HD	macro	2.4 hours
<i>Total</i>					7.15 hours
left capitate	1	10/9/8	medium HD	macro	2.3 hours
left capitate	2	9	medium HD	macro	1.3 hours
left capitate	3	7	medium HD	macro	1.9 hours

(Table 4 continued)

Bone	Scan Attempt	Divisions	Definition	Range	~Time Spent
				<i>Total</i>	5.5 hours
axis	1	7/8	medium HD	macro	7.8 hours
right ulna	1	7	medium HD	macro	4.3 hours
left scaphoid	1	8	medium HD	macro	1 hour
right third metacarpal	1	8	medium HD	macro	1.8 hours
				Total	124.45 hours

number of divisions. For example, 68% of the computer's memory will be used to scan in seven divisions, 78% in eight divisions, 88% in nine divisions, and so forth.

Table 5. Points per Square Inch

Mode	Definition	Range	Points/in <sup>2</sup>
360°	high HD	macro	160,000
360°	medium HD	macro	40,000
360°	high HD	wide	17,000
360°	medium HD	wide	4,400

After experiencing much difficulty scanning in high HD, a "point" experiment was conducted to see: 1) the total number of points generated in a high HD macro range scan and wide range scan, 2) the total number of points produced in a medium HD macro range scan and wide range scan, and 3) how much the number of divisions affects the number of points. The object scanned was the shaft of the left humerus from Moho Cay burial 4. See Table 6 below for the results.

Table 6. Point Experiment

Mode	Divisions	Definition	Range	Total # of Points
360°	7	high HD	macro	3,320,562
360°	7	high HD	wide	2,303,612
360°	9	medium HD	macro	1,059,535
360°	7	medium HD	macro	825,066
360°	9	medium HD	wide	661,585
360°	7	medium HD	wide	555,529

### Visibility of Features

All of the bones in the present sample have varying degrees of exposed trabecular bone somewhere on the element. Regrettably, the NextEngine has difficulty capturing trabecular bone. As a result, missing data (holes) occur where the trabecular bone is exposed. Ultimately, every feature, with the exception of the nutrient foramen is well-pronounced on the 3D models. While scanning, I observed that the nutrient foramen was successfully captured in single and bracket mode. However, when multiple rotations were introduced, the nutrient foramen was essentially buried in a sea of polygons. Additionally, certain angles and crevices were difficult to capture and often resulted in a combination of missing data and overlapping data. This result can be seen on the lateral and palmar views of the left capitate (Figures 13 and 14), the foramina of the axis (Figures 15, 16, 17, and 18), and the left scaphoid (Figure 24).

## Discussion

### Learning Curve of 3D Technologies

Some of the industries that use 3D imaging include aerospace, automotive, medical, civil engineering, reverse engineering, art, design, manufacturing, entertainment, and architecture. Naturally, each industry's preferred 3D scanner and software program will result in their own specific learning curve. Depending on one's project in bioarchaeology or museum research, one could use several different types of software programs. As explained by Metallo and Rossi (2011:65), one shortcoming of 3D technologies is the learning curve:

The time investment required in learning how to operate the hardware and software applicable to one set of objects or collections may not work for the next. Adapting tools and techniques from diverse industries requires a patchwork of software not necessarily designed to play nice together. In one current project we found ourselves using three different software packages formerly reserved for the mining industry, reverse engineering, and rendering/animation.

When I began working at the DIVA Lab in August 2012 as part of my graduate assistantship responsibilities, I had no prior experience with 3D scanners and 3D scanning software. Nevertheless, I quickly grasped the basics of the NextEngine and ScanStudio software during a single two-hour session. To be clear, the "basics" to which I am referring include setting up the NextEngine, preparing a test scan, and becoming comfortable with ScanStudio's user interface so that one can trim, align, fuse separate scans, fill holes, and generally manipulate the 3D model. However, some 3D technologies have a rather long learning curve. Even though I easily understood the basics of the NextEngine and ScanStudio, I still experiment with the scan settings and post-processing procedures to figure out how to best produce the desired results.



The first time I scanned an object larger than a ceramic bowl was when I scanned the right femur from Wild Cane Cay burial 3. This time was also my first experience scanning bone. As I scanned, I developed the beginning of a standard methodology, which began the scanning process at the distal portion of the femur and proceeded along the bone to the proximal end. When I scanned the right femur a second time, I added to the methodology by aligning scan families after each scan. In addition, I learned to use single/bracket scans to image crevices and foramina missed during a 360-degree scan. I was comfortable and confident with the process after I scanned the femur for a second time. The third time I scanned the left humerus from Moho Cay burial 4, I amended the methodology to include trimming extra data not needed for alignment. I continued to use this methodology throughout the remainder of the project. However, each bone provided a new set of issues to overcome, including, difficulty capturing crevices, foramina, and trabecular bone. In addition, each bone had to be carefully positioned in order to capture data, so the process of 3D imaging is far from automatic. Often a specific bone was rescanned multiple times. Typically, the time spent scanning and post-processing was less than the previous time (see Table 3). Overall, I learned that 3D scanning involves a lot of trial and error. Indeed, Metallo and Rossi (2011:65) note, "There is no 'how-to' book on 3D digitizing of museum collections." Similarly, there is no standardized method of 3D scanning among anthropologists. Fortunately, my time scanning was during my graduate assistantship in the LSU DIVA lab, while I also was supervising undergraduates.

### **Limitations of 3D Scanning**

The learning curve for 3D surface scanning will vary by person and technology. Regardless, a time investment is required, both in learning the technologies and in practice.

In this paper, I documented the time required for NextEngine scan modes (see Table 1) as well as the time I spent scanning and post-processing each bone (see Table 3). Even when the computer and software programs are running smoothly, the process of scanning and post-processing is undeniably time-consuming. Indeed, many researchers have noted the time-consuming nature of 3D scanning (Davies et al. 2012; Fourie et al. 2011; Kuzminsky and Gardiner 2012; McKillop and Sills 2013a; Metallo and Rossi 2011; Noldner and Edgar 2013; Sholts et al. 2010; Sumner and Riddle 2009).

As 3D scanning gains in popularity, 3D scanning systems are becoming readily available with varying costs. Kuzminsky and Gardiner (2012:2749) note that “3D laser scanners offer one of the most affordable options that museum curators and researchers can employ to preserve skeletal collections and create large databases to share.” However, there are other aspects to consider. For example, as I discussed earlier in the results section, I experienced technical difficulties while working in ScanStudio HD PRO.

Computers running 3D imaging software need more than a high-powered CPU and lot of RAM to run smoothly. A high-quality video card is absolutely necessary, especially when displaying detailed objects. Although the specifications of the computers I used in my study exceed the minimum requirements for ScanStudio, large image files tended to crash the computer. Even though both computers had video cards for graphics work, better video cards are needed for large image files and in particular for post-processing, including fusing separate scan families. Both computers I used exceed the minimum requirements of 4 gigabytes of RAM for ScanStudio HD (<http://www.nextengine.com/products/scanstudio-hd/specs/system-requirements>; see Table 7 below). The Lenovo desktop used in this study has 12 gigabytes of RAM. The Samsung laptop has 8 gigabytes of RAM (see Table 3).

Nonetheless, I still received a low RAM warning on the Samsung laptop. Both computers have a quad-core central processing unit, which exceeds the recommended requirements to run ScanStudio. Ultimately, the cost of 3D technology and what is required to use the technology adds up, especially for a variety of materials of various sizes.

Table 7. ScanStudio HD System Requirements

Minimum	Recommended
Windows XP/Vista/7	Windows XP 64 / 7 64-bit
2 GHz CPU	2.5 GHz Dual-Core CPU
3 GB RAM	4 GB RAM
256 MB Graphics	512 MB Graphics

Long-term storage and preservation of 3D digital images is important to consider. Metallo and Rossi (2011:65) address the reality of changing file types: “If museums worry about the longevity of a file format as common as a .jpeg from a digital camera, what about the slew of obscure and specialized file types for 3D?” Indeed, these are questions a museum and/or research institution must consider before embarking upon the task of creating a 3D digital collection.

### **Benefits of 3D Scanning and 3D Digital Archives**

Archaeological skeletal material is fragile. A permanent 3D digital archive would prevent the bones from any further breaks and/or loss of bone during research thereby preserving and conserving the skeletal material. A 3D digital collection can also be studied remotely. Of additional note, the host country of archaeological excavations will often not allow archaeologists to travel outside of the country with archaeological material or skeletal remains. An alternative solution to this issue is to bring a 3D scanner to the site so

that the archaeologist can scan artifacts and bone. Scanning can even be done in situ (see Tucker 2012). When the archaeologist returns to their institution, they will have accurate 3D digital models from which they can study (McKillop and Sills 2013a).

### **Conclusions about Feasibility**

Previous 3D imaging by other researchers indicates the accuracy of NextEngine scans to be high (Davies et al. 2012; Noldner and Edgar 2013; Sholts et al. 2010). After aligning scan families, ScanStudio reports the accuracy of the alignment. Every alignment in this study is accurate to 0.001". Furthermore, the NextEngine captures detail and images small objects. As I discussed, there the scanner must wait as the NextEngine scans (see Table 1). However, if multiple computers and NextEngines are available, the scanning operator can simultaneously scan two or more objects each on a different NextEngine. In fact, as a Graduate Assistant in the LSU DIVA Lab, I often imaged pottery sherds on two separate NextEngines. The NextEngine is portable and easy to learn and use. Ultimately, the NextEngine is great for scanning small archaeological or skeletal collections as well as selective scanning, making the NextEngine a valuable tool to museums and research institutions.

## **Conclusion**

As scientists, we need to closely explore 3D imaging technology because 3D methods are being used more frequently. 3D scanning is still relatively new to the field of Anthropology. Nevertheless, research projects in Archaeology and Biological Anthropology have used 3D laser surfacing scanning technology to assess biomechanical properties of bones, to digitally reconstruct fragmented bones, to examine muscle insertion sites on bones, to calculate surface area, volume, and angles, and to take measurements of the digital model. However, 3D digital databases cannot replace past research and resources. Instead, 3D imaging enhances our research and offers a new tool for researchers. Ultimately, the purpose of my thesis research is to illustrate the value of 3D imaging technology to the fields of archaeology and biological anthropology as well as for archiving and sharing material in museums.

## References

- Davies, Thomas G., Colin N. Shaw, and Jay T. Stock  
2012 A Test of a New Method and Software for the Rapid Estimation of Cross-Sectional Geometric Properties of Long Bone Diaphyses from 3D Laser Surface Scans. Archaeological and Anthropological Sciences 4:277-290.
- Dawson, Peter, Richard Levy, and Natasha Lyons  
2011 "Breaking the Fourth Wall": 3D Virtual Worlds as Tools for Knowledge Repatriation in Archaeology. Journal of Social Archaeology 11:387-402.
- Fourie, Zacharias, Janalt Damstra, Peter O. Gerrits, and Yijin Ren  
2011 Evaluation of Anthropometric Accuracy and Reliability Using Different Three-Dimensional Scanning Systems. Forensic Science International 207:127-134.
- Gilissen, Emmanuel  
2009 Museum Collections, Scanning, and Data Access. Journal of Anthropological Sciences 87:223-226.
- Hawkey, Diane E. and Charles F. Merbs  
1995 Activity-induced Musculoskeletal Stress Markers (MSM) and Subsistence Strategy Changes among Ancient Hudson Bay Eskimos. International Journal of Osteoarchaeology 5:324-338.
- Kuzminsky, Susan C., and Megan S. Gardiner  
2012 Three-Dimensional Laser Scanning: Potential Uses for Museum Conservation and Scientific Research. Journal of Archaeological Science 39:2744-2751.
- McKillop, Heather  
2004 The Classic Maya Trading Port of Moho Cay. In The Ancient Maya of the Belize Valley: Half a Century of Archaeological Research. James F. Garber, ed. pp. 257-272. Gainesville, FL: University Press of Florida.  
  
2005 In Search of Maya Sea Traders. College Station, TX: Texas A&M University Press.
- McKillop, Heather, and E. Cory Sills  
2013a Sustainable Archaeological Tourism of the Maya Paynes Creek Project Using 3D Technology. Anthropology News. <http://www.anthropology-news.org/index.php/2013/02/06/sustainable-archaeological-tourism-of-the-underwater-maya-project-by-3d-technology>, accessed March 7, 2014.  
  
2013b Sustainable Archaeological Tourism of the Underwater Maya Salt Works in Paynes Creek National Park. Research Reports in Belizean Archaeology 10:289-296.

Metallo, Adam, and Vince Rossi

2011 The Future of Three-Dimensional Imaging and Museum Applications. Curator: The Museum Journal 54(1):63-69.

Noldner, Lara K., and Heather J. H. Edgar

2013 3D Representation and Analysis of Enthesis Morphology. American Journal of Physical Anthropology 152:417-424.

Sholts, Sabrina B., Sebastian K.T.S. Wärmländer, Louise M. Flores, Kevin W.P. Miller, and Phillip L. Walker

2010 Variation in the Measurement of Cranial Volume and Surface Area Using 3D Laser Scanning Technology. Journal of Forensic Sciences 55:871-876.

Sumner, T. Alexandra, and Andrew T.R. Riddle

2009 Remote Anthropology: Reconciling Research Priorities with Digital Data Sharing. Journal of Anthropological Sciences 87:219-221.

Tucker, Abigail

2012 How Two Laser Cowboys Saved the Day. Smithsonian, June 2012, <http://www.smithsonianmag.com/arts-culture/How-Two-Laser-Cowboys-Saved-The-Day.html#>, accessed December 17, 2013.

Waibel, Günter

2013 About Smithsonian X 3D. <http://3d.si.edu/about>, accessed December 17, 2013.

Weber, Gerhard W. and Fred L. Bookstein

2011 Virtual Anthropology: A Guide to a New Interdisciplinary Field. Austria: Springer-Verlag/Wein.

White, Tim D., Michael T. Black, and Pieter A. Folkens

2012 Human Osteology. 3rd edition. San Diego, CA: Elsevier.

## **Vita**

Karen Leigh Beebe received her bachelor's degree at Millsaps College in 2008. Thereafter, she worked as a photo editor and assistant at a photography studio in Jackson, Mississippi. Seeking a new challenge, she made the decision to enter graduate school in the Department of Geography and Anthropology at Louisiana State University and received a graduate assistantship. For three semesters, she was assigned to work in her advisor's lab, the LSU Digital Imaging and Visualization in Archaeology (DIVA) Lab. Her duties included supervising undergraduates in 3D scanning, keeping records of 3D images, and doing 3D scanning of a variety of artifacts. She expects to receive a M.A. in Anthropology in May 2014. After graduation, she would like to continue 3D imaging skeletal material, artifacts, or other objects at a museum, other research institution, or the private sector.